

Article

Assessing the Impacts of COVID-19 on SO₂, NO₂, and CO Trends in Durban Using TROPOMI, AIRS, OMI, and MERRA-2 Data

Boitumelo Mokgoja ¹, Paidamwoyo Mhangara ^{1,*} and Lerato Shikwambana ^{1,2}

¹ School of Geography, Archaeology and Environmental Studies, University of the Witwatersrand, Johannesburg 2050, South Africa; 1747888@students.wits.ac.za (B.M.); lshikwambana@sansa.org.za (L.S.)

² Earth Observation Directorate, South African National Space Agency, Pretoria 0001, South Africa

* Correspondence: paida.mhangara@wits.ac.za

Abstract: This research report investigated the impacts of the COVID-19 lockdown restrictions on CO, SO₂, and NO₂ trends in Durban from 2019 to 2021. The COVID-19 lockdown restrictions proved to decrease greenhouse gas (GHG) emissions globally; however, the decrease in GHG emissions was for a short period only. Space-borne technology has been used by researchers to understand the spatial and temporal trends of GHGs. This study used Sentinel-5P to map the spatial distribution of CO, SO₂, and NO₂. Use was also made of the Atmospheric Infrared Sounder (AIRS), Modern-Era Retrospective Analysis for Research and Applications, Version 2 (MERRA-2), and the Ozone Monitoring Instrument (OMI) to understand the temporal trends of CO, SO₂, and NO₂, respectively. To validate the results of this study, we used the Sequential Mann–Kendall (SQMK) test. This study indicated that there were no significant changes in all the investigated gases. Therefore, this study failed to reject the null hypothesis of the SQMK test that there was no significant trend for all investigated gasses. Increasing trends were observed for CO, SO₂, and NO₂ trends during winter months throughout the study period, whereas a decreasing trend was observed in all investigated gases during the spring months. This shows that meteorological factors play a significant role in the accumulation of air pollutants in the atmosphere. Most importantly, this study has noted that there was an inverse relationship between the trends of all investigated gases and the COVID-19 lockdown restrictions.

Keywords: COVID-19; SQMK; AIRS; OMI; MERRA-2; Sentinel-5P; lockdown measures; SDIB



Citation: Mokgoja, B.; Mhangara, P.; Shikwambana, L. Assessing the Impacts of COVID-19 on SO₂, NO₂, and CO Trends in Durban Using TROPOMI, AIRS, OMI, and MERRA-2 Data. *Atmosphere* **2023**, *14*, 1304. <https://doi.org/10.3390/atmos14081304>

Academic Editors: Chong Wei, Chong Shi, Nan Li and Xingjun Xie

Received: 18 July 2023

Revised: 11 August 2023

Accepted: 14 August 2023

Published: 17 August 2023



Copyright: © 2023 by the authors. Licensee MDPI, Basel, Switzerland. This article is an open access article distributed under the terms and conditions of the Creative Commons Attribution (CC BY) license (<https://creativecommons.org/licenses/by/4.0/>).

1. Introduction

Cities are the greatest emitters of anthropogenic emissions; they consequently result in increased air temperatures in many urban areas [1,2]. Air pollution accounts for over six million deaths per annum globally [3,4]. Further, increased rates of pollution drive ecosystem deterioration and health risks [5]. As a result, people and animals are affected. For example, people may become susceptible to respiratory, heart, and lung diseases [5–7], whereas animals may experience death, physiological tension, and disease [8]. In 2021, Western Europe and North America experienced flood and extreme heat events, respectively, which were ascribed to human-induced climate change effects [9]. Even when measures are placed to regulate emissions, the emissions persistently increase. Global carbon dioxide (CO₂) emissions increased to 36.64 GtCO₂ in 2019, and then a sudden decrease of 1.98 GtCO₂ occurred in 2020 in response to the coronavirus disease (COVID-19) pandemic [9]. However, the UNEP [9] has noted that the global decrease in emissions from COVID-19 was only short-term. The pandemic affected the cost and demand for global oil [10], mainly because most industrial activities were curtailed and there was limited fossil fuel combustion. Consequently, there was a global 30% reduction in NO₂ [9]. Emissions from transport, manufacturing factories, and mines were affected as COVID-19 emerged in South Africa and the rest of the world. Consequently, countries implemented

lockdown measures to control and reduce the COVID-19 infection rate, which resulted in people's movements being restricted. Simultaneously, mining, transport, and numerous industries were halted [1,6,11]. Owing to lockdowns, there was a 17% daily decrease in CO₂ in 69 countries [12]. Additionally, NO₂ was also reduced by 60% in 34 country regions. The decrease in NO₂ is mostly attributed to the restrictions imposed on transport since it is responsible for most NO₂ abnormalities in the 34 countries mentioned in [4]. Bashir et al. [13] noted that COVID-19 provided the environment with time for healing. In other words, this shows that COVID-19 had a significant positive impact on GHG emissions across the world. However, the implementation of measures to control COVID-19 infections exacerbated the decline in the global economy to an even greater extent than occurred due to World War 2 [12]. Given that countries are bound to recover from the economic ramifications of COVID-19, the UNEP [9] suggests that while countries are recovering economically, they should incorporate decarbonisation strategies.

Durban is one of South Africa's industrial cities. It has numerous economic activities including chemical industries, shipping, car manufacturing, and logistics. Furthermore, it provides a home to the two largest petroleum refineries in the country: namely SAPREF and Engen [2,14,15]. Consequently, Durban is responsible for supplying over 58% of South Africa's petroleum [2,14,16]. Additionally, it is also home to Africa's busiest port [2,14]. Manqele [15] showed that Durban is responsible for over 60% of South Africa's exports and imports conducted from the Durban Port. In a similar vein, the South Durban Industrial Basin (SDIB) is understood to be the economic hub of Kwa-Zulu Natal [15]. Petroleum refineries, sugar refineries, paper manufacturing factories, and agricultural combustion in Durban account for over 980 000 million tonnes per year of trace gases [17]. Emissions from light vehicles in Durban contribute 43% of road transport emissions, which is 12% greater than the national level, as argued by Jagarnath and Thambiran [2]. With the global COVID-19 outbreak (in March 2020 in South Africa), according to Potgieter et al. [18], industries including manufacturing and transport were curtailed to control the spread of the virus. Consequently, there was a significant reduction in emissions globally [5]. The implemented lockdowns curtailed most economic activities, which resulted in energy consumption reduction [12]. Owing to the abysmal regulations of emissions, anthropogenic-induced climate change continues to exacerbate [19]. Therefore, proper management of emissions is needed to abate the ramifications of climate change. This study's focus is on CO, SO₂, and NO₂ emissions because these gases pose threats to human health, environment, and climate [20,21]. This paper aims to understand the Impacts of COVID-19 lockdown restrictions on SO₂, NO₂, and CO column densities in Durban. We will use AIRS, MERRA-2, and OMI data for temporal column densities for CO, SO₂, and NO₂, respectively. Sentinel-5p will be used to map the spatial distribution of the investigated gases.

2. Materials and Methods

2.1. Study Site

Durban is a city in the province of Kwa-Zulu Natal (KZN) in South Africa (see Figure 1). It occupies a 2297 km² area of land and has a population of approximately 3.7 million [2,14]. Durban is the third-largest city in Africa [14]. The city is situated on the eastern side of South Africa and is, therefore, adjacent to the Indian Ocean. Furthermore, it is a wet area that experiences over 1000 mm of precipitation annually, and it is usually wet in summer and dry in winter [15]. Manqele [15] notes that the wind speed in Durban is at its minimum in the winter months compared to the summer months. Durban is known for industrial activities, including manufacturing and shipping. As a result, it has the busiest port in Africa and the two largest petroleum refineries in South Africa [2,15,16]. The South Durban Industrial Basin (SDIB), situated to the south of the city, has the largest number of petroleum refineries in the entire country; thus, it is considered an economic hub of KZN [15]. Additionally, Durban is the largest producer of vehicles in South Africa [2]. As noted in [14], the busy port is the conduit for high transportation volumes. Consequently, road traffic can be expected to be significant as a result of the transportation of goods

from the Durban Port to the market. The prevailing southwesterly winds in the city of Durban [22] are likely to affect the dispersion of air pollutants across Durban.

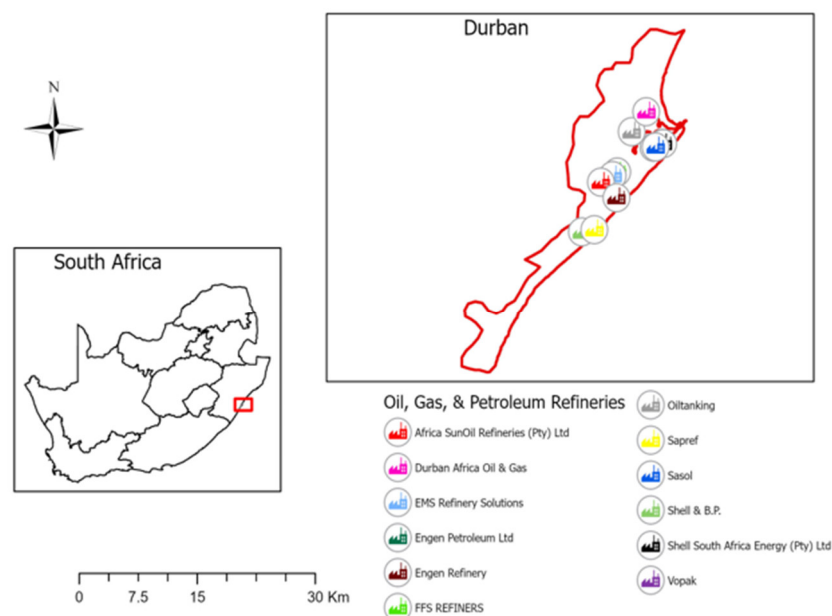


Figure 1. Durban, KZN, and South Africa, along with the respective oil, gas, and petroleum refineries.

2.2. SENTINEL-5P/TROPOMI

Sentinel-5 precursor (5P) is a satellite developed by the European Space Agency, which comprises Italy, the United Kingdom, Spain, Germany, and 19 other European countries [23]. Sentinel-5P was launched into space on 13 October 2017 with a dedicated mission to carry out monitoring of UV radiation, air quality, ozone, and climate [23,24]. This spaceborne technology has TROPOMI, which permits measurements of various atmospheric gases including CO, SO₂, NO₂, ozone (O₃), formaldehyde (CH₄O), and methane (CH₄). TROPOMI/Sentinel-5 has a spatial resolution of 3.5 × 7 km², making it 13 times more advanced than the OMI [23,24]. Furthermore, TROPOMI was developed with advanced retrieval algorithms; as a result, TROPOMI is recommended for improved detection of micro SO₂ plumes compared to the OMI [23]. Furthermore, this sensor is made up of seven spectral bands: ultraviolet and visible 1 (UV-1) (270–300 nm), UV-2 (300–370 nm), visible (VIS) (370–500 nm), near-infrared 1 (NIR-1) (685–710 nm), NIR-2 (745–773 nm), shortwave infrared 1 (SWIR-1) (1590–1675 nm), and SWIR-3 (2305–2385 nm). Sentinel-5P has a swath width of 2 600 km, permitting the sensor to provide global coverage [11,23]. Moreover, the sensor has a superb temporal resolution with less than a day's revisit time [23]. This means that TROPOMI can pass by a certain area twice a day. This research report utilised TROPOMI for CO, SO₂, and NO₂ spatial data based on the sensor's excellent spatial resolution. Sentinel-5P data were obtained from <https://code.earthengine.google.com/> (accessed on 15 August 2023), the Google Earth Engine site. These data were in the form of Level 2 data, which means that they were atmospherically corrected using various retrieval and analysis algorithms. Lastly, Sentinel-5P data were further manipulated using ArcGIS 10.2 to create maps to show the spatial distribution of NO₂, SO₂, and CO.

2.3. OMI

An instrument in the Earth Observing System (EOS), the OMI was launched in July 2004 by the Netherlands Agency for Aerospace (NIVR) in partnership with the Finnish Meteorological Institute (FMI). This sensor was developed to continue the duties of the Scanning Imaging Absorption Spectrometer for Atmospheric Cartography (SCIAMACHY) and the Global Ozone Monitoring Experiment [25]. Furthermore, it has continued to record the total column ozone and recording trace gases [26]. This sensor has three spectral bands:

UV-1; 269–309 nm, UV-2; 310–367 nm, and visible; 269–500 nm, which enables the sensor to record products such as O₃, SO₂, NO₂, formaldehyde (HCHO), bromine oxide (BrO), and aerosols [27]. These gases are displayed at a decent spatial resolution of 13 × 25 km². Moreover, the OMI has a swath width of 2600 km and a one-day temporal resolution (that is, it enables global coverage in one day) [26–28]. According to Levelt et al. [25], the OMI has advanced NO₂ retrieval algorithms, which is why we used the OMI for NO₂ time series data in Durban. These data were obtained from Giovanni's website (<https://giovanni.gsfc.nasa.gov/giovanni/>), (accessed on 15 August 2023), which is evaluated and maintained by the National Aeronautics and Space Administration (NASA).

2.4. AIRS

AIRS is one of the satellites of the EOS that was launched in May 2002. This sensor was developed by the British Aerospace System (BAE). The purpose of this sensor is to address surface temperature, water cycle, climate change, and GHGs [24,29,30]. AIRS has three spectral bands: 3.75–4.61 μm, 6.20–8.22 μm, and 8.8–15.44 μm, and over 2000 channels [30]. Further, this sensor is made of a 45 km horizontal spatial resolution at the nadir and a 2 km vertical spatial resolution [29]. AIRS has a swath width of 1600 km and a one-day frequency temporal resolution, which allows for near global coverage per day [24]. This sensor offers various products including O₃, CO, methane (CH₄), air temperature, surface temperature, and aerosols. Additionally, AIRS has advanced measurement precision and accuracy [30]. For that reason, we will use this sensor to assess the CO time series trends in Durban. AIRS data were obtained from Giovanni (<https://giovanni.gsfc.nasa.gov/giovanni/>, (accessed on 15 August 2023)). The data came in Level 2B, which means that the data were extracted from Level 1B, therefore, atmospheric and radiometric corrections were already performed.

2.5. MERRA-2

MERRA-2 is a reanalysis data that integrates EOS satellites and Goddard EOS, version 5 (GEOS-5). MERRA reanalysis was succeeded by MERRA-2 with advanced GEOS-5 [31]. This reanalysis data measured wind speed, surface temperature, air temperature, and GHGs from the early 1980s [32]. MERRA-2 uses a cubed sphere grid with a 0.5° × 0.625° latitude by longitude spectral resolution [33,34]. These data came in Level 2B. GEOS-5 has introduced improved retrieval algorithms and analysis algorithms into the MERRA family [33]. This is evident as the (now MERRA-2) reanalysis can assimilate aerosols as opposed to the MERRA reanalysis, which could not [34]. Based on these technological advancements, the current study used these reanalysis data to determine SO₂ time series trends in Durban. MERRA-2 reanalysis data were obtained from Giovanni (<https://giovanni.gsfc.nasa.gov/giovanni/>, (accessed on 15 August 2023)).

2.6. SQMK

The Sequential Mann–Kendall (SQMK) test was initially introduced by Sneyers [24]. The test was proposed to validate time series trends. It is used to detect sudden changes in the time series [24,35–37]. The SQMK test is made up of two series, named progressive and retrograde, which are also known as forward series $u(t)$ and backward series $u'(t)$, respectively. When the $u(t)$ series and $u'(t)$ series cross and proceed to diverge to surpass the threshold, it is an indication of a significant statistical trend [24,35,36]. The null hypothesis of this test states that there is no significant trend, whereas the alternative hypothesis states that there is a significant trend. The threshold value of this study was set to ±1.96 ($p = 0.05$). The crossing point of the two series depicts the year in which the trend started [36]. This test is set out in the following manner.

For every comparison, the number of cases $x_a > x_b$ is included and denoted by n_a , where x_a (1, 2, 3, . . . n) and x_b (1, 2, 3, . . . n–1) are considered the sequential values in a series, respectively.

The test statistic t_i is calculated by:

$$t_a = \sum_b^a n_b \tag{1}$$

The mean $E(t)$ and the variance $var(t_i)$ of the test statistic are calculated by:

$$E(t) = \frac{n(n-1)}{4} \tag{2}$$

$$var(t_a) = \frac{a(a-1)(2a+5)}{72} \tag{3}$$

The sequential progressive value can be calculated as:

$$u(t) = \frac{t_a - E(t)}{\sqrt{var(t_a)}} \tag{4}$$

3. Results

3.1. Spatial Distribution Analysis

3.1.1. CO

COVID-19 transitioned the global paradigms by curtailing industries, transport, and other major economic activities. Ref. [13] argue that COVID-19 awarded the environment a period of recuperation. This comes from the sense of curbing transport and industries resulted in a reduction in GHGs emissions, as stated by Bashir et al. [13]. Sentinel-5p was used to show the spatial distribution of all investigated gases. Figures 2–4 show seasonal CO column density measurements in Durban from 2019 to 2021. Summer is represented by December–January–February (DJF), autumn by March–April–May (MAM), winter by June–July–August (JJA), and lastly, spring is represented by September–October–November (SON). Figure 2 shows that 2019 had significant CO hotspots compared to 2020 (see Figure 3). Additionally, the areas to the north of Durban (north Durban) had insignificant CO column density compared to the areas to the south of Durban (south Durban). This is mainly because south Durban is recognised as the economic hub of KZN as it hosts numerous industries, whereas north Durban has relatively little industry and is primarily residential [38]. The summer, autumn, and spring of 2019 showed high CO column density compared to the winter of 2019 (see Figure 2). The observed decrease in CO column density in the winter of 2019 could have been due to better air pollution control and a substantial increase in CO sink availability. In contrast, a major decrease in CO column density was observed in the summer of 2020 compared to the summer of 2019 (see Figures 3a and 2a, respectively). Relative to the autumn of 2019, the comparatively big decrease continued in the autumn of 2020 (see Figures 2b and 3b). This decrease can be attributed to the Level 5 lockdown, which occurred from 26 March 2020 to 30 April 2020 (see Table 1). Level 5 was known as the “hardest lockdown”, meaning that the majority of the economic activities were not operational. Therefore, as the levels eased from Level 5 to lower levels, some economic activities were allowed to operate based on their significance to the society and economy [18].

Table 1. South African lockdown levels, dates, and restrictions [18,39].

Lockdown Levels	Dates	Restrictions
Level 5	26 March 2020 to 30 April 2020	Only essential services were permitted to operate; transport was restricted, and only the transportation of goods was allowed; mining, manufacturing factories, industries, and other economic activities were at a halt.

Table 1. Cont.

Lockdown Levels	Dates	Restrictions
Level 4	1 May 2020 to 31 May 2020; 16 June 2021; 28 June 2021 to 25 July 2021	Some sectors were allowed to operate with limitations; mining, tourism, and flights remained inactive; all borders were not operating; however, designated ports were operating; cargo, fuel, and goods transportation was allowed; public transportation was allowed to operate with fewer restrictions.
Level 3	1 June 2020 to 17 August 2020; 29 December 2020 to 28 February 2021; 16 June 2021 to 27 June 2021; 26 July 2021 to 12 September 2021	More sectors were allowed to operate; global business services and tourism started functioning; inter-provincial movement was at a halt; international flights were not allowed.
Level 2	18 August 2020; 31 May 2021 to 15 June 2021; 13 September 2021 to 30 September 2021	Local air travel was unbanned; inter-provincial travel was allowed; significant economic activities started operating, including mines and manufacturing industries; all modes of transportation were permitted.
Level 1	21 September 2020 to 28 December 2020; 1 March 2021 to 30 May 2021; 1 October 2021 to Present	Economic activities were allowed to operate on a normal basis; travelling of all types was permitted (except in 2020, travelling was still limited, and many economic activities were still at a halt).

Industrial, manufacturing, and transport activities were severely curtailed; therefore, there were few operational sources of CO. The winter of 2020 showed a significant CO hotspot in south Durban (see Figure 3c). This coincided with Level 5 lockdown measures being eased to Level 4. Therefore, some economic activities were permitted to recommence operation (see Table 1). Oil refineries and petroleum refineries were considered essential, and, therefore, they were relieved of the Level 5 lockdown measures [40]. It can be argued that oil and petroleum refineries may have contributed to the CO hotspot observed in the winter of 2020 (see Figure 3c). The hotspot is observed at the location of numerous refineries (see Figure 1). Additionally, low wind speed and low temperature may have played a role in influencing CO to be trapped in the atmosphere. A further increase in CO continued in the spring of 2020 (see Figure 3d). This can be attributed to the further easing of lockdown restrictions from Level 4 to Level 3, at which point more sectors were permitted to operate and road transport was less restricted (see Table 1). Figure 4a shows that the summer of 2021 had a slight increase in CO column density in north Durban but a notable increase in the far south of Durban.

Additionally, a slight increase in CO column density occurred near the harbour, which can be attributed to the operation of heavy-duty vehicles. Industries, mills, and factories near the harbour, such as Illovo Sugar Africa and Tata Chemical Industry, may have contributed to the increase in CO column density observed in Figure 4a. The transportation of goods may also account for the increase in CO column density in the summer of 2021 since transportation of goods was regarded as an essential service. An increase was observed in the autumn of 2021 in the SDIB, as it showed a more pronounced CO hotspot spreading to the northeast (see Figure 4b). This can be attributed to the easing of lockdown levels from Level 3 to Level 1. By that stage, most economic activities were allowed to operate (see Table 1). South Africa was under Level 3 and Level 2 lockdown restrictions for most of the winter of 2021, and a significant increase in CO column density is observed in Figure 4c. This could have been due to low temperatures in winter, which are characterised by low solar insolation, which reduces the photochemical reaction of CO gas, and the dominance of anticyclone circulation of air in Durban, which causes air to sink [17,22].

Consequently, this traps CO pollutants in the atmosphere. Furthermore, natural sources mentioned in Chapter 2 may have played a role in the increase in CO accumulation. A slight hotspot occurred near the harbour in winter 2021 (see Figure 4c). This may have been due to transport emissions since all modes of transport were by then permitted, including water transport. This also means exports and imports were permitted; therefore,

heavy-duty vehicles were actively operating near the harbour. The spring of 2021 had a more pronounced CO hotspot in the SDIB compared to the winter of 2021 (see Figure 4d,c). However, CO column density was not as widespread in the spring of 2021 as in the winter of 2021 (see Figure 4d,c, respectively). Air pollutants settle near their sources in winter and the conditions, therefore, allow them to accumulate. In contrast, the high intensity of winds in spring allows air pollutants to travel away from their sources relatively fast; as a result, there is less air pollutant accumulation compared to winter [22].

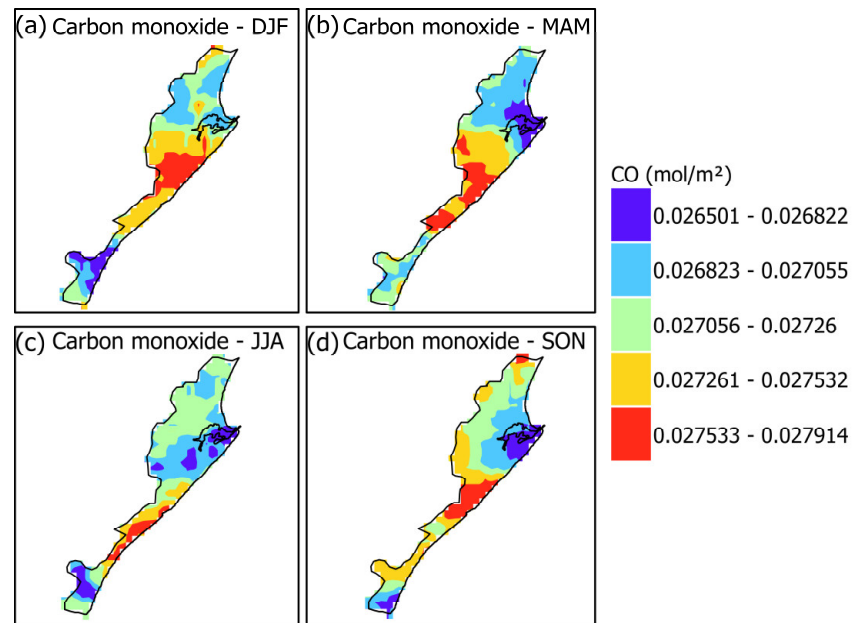


Figure 2. Carbon monoxide column density during (a) DJF (December–January–February), (b) MAM (March–April–May), (c) JJA (June–July–August), and (d) SON (September–October–November) for 2019.

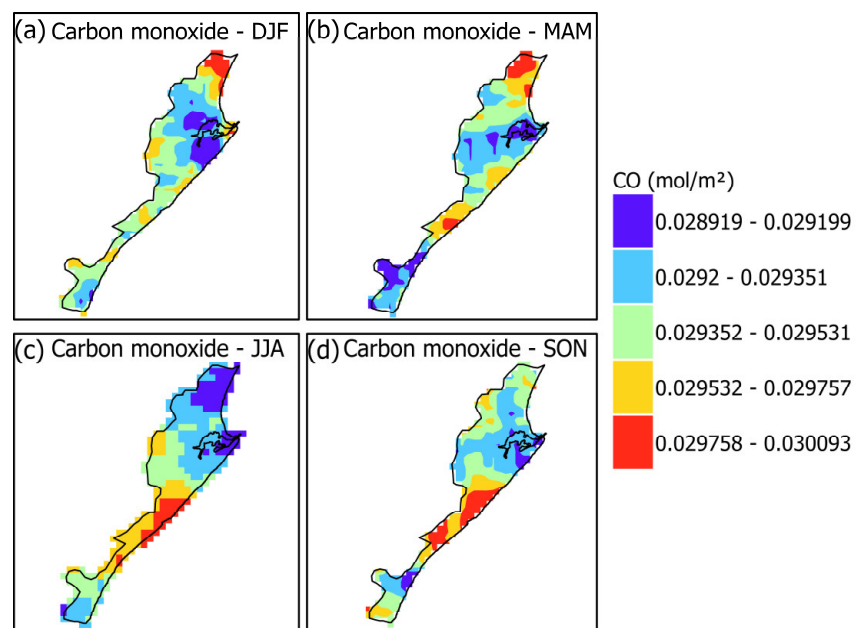


Figure 3. Carbon monoxide column density during (a) DJF (December–January–February), (b) MAM (March–April–May), (c) JJA (June–July–August), and (d) SON (September–October–November) for 2020.

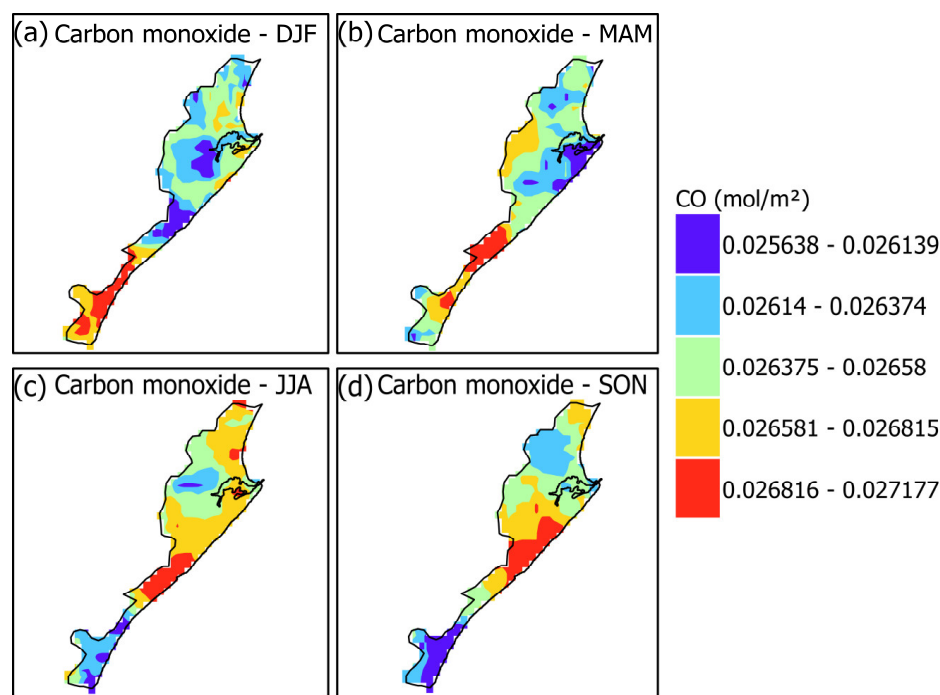


Figure 4. Carbon monoxide column density during (a) DJF (December–January–February), (b) MAM (March–April–May), (c) JJA (June–July–August), and (d) SON (September–October–November) for 2021.

3.1.2. SO₂

SDIB has significant industrial capacity Diab et al. [7]. This includes oil refineries, sugar mills, petroleum refineries, paper manufacturers, and chemical industries. With that being noted, it can be expected that trace gases will reach higher concentrations in south Durban than north Durban. However, Figure 5a shows that the summer of 2019 had significant SO₂ hotspots in north Durban. The increase in SO₂ column density in north Durban could have been due to road transportation, the operation of light industries, and various sources of domestic fuel combustion. Additionally, relatively less gusty winds that dominate the north of Durban may have contributed to the higher accumulation of SO₂ column density. Ref. [41] argued that south Durban has relatively high wind velocity and temperature compared to north Durban. Therefore, the dispersion of air pollutants and photochemical reactions in north Durban is lower than in south Durban. Hotspots of high SO₂ concentrations are observed at the Port of Durban during the autumn of 2019, as shown in Figure 5b. This could mean that the port was highly active, including heavy-duty vehicles operating. In addition, factories may have also contributed to the observed high SO₂ column density, as [17] argued that there are factories surrounding the Port of Durban. Winter meteorological factors, such as low wind speed and low temperatures, may have played a role by trapping SO₂ pollutants within the atmosphere in the winter of 2019, hence the increased SO₂ column density (see Figure 5c). The spring of 2019 shows a major SO₂ column density increase in north Durban compared to south Durban (see Figure 5d). This increase could be the result of increased humidity during the spring months. This is mainly because there would have been more water vapour in the air, which would limit air circulation [22].

As a result, air circulation becomes much slower, and, therefore, air particles are forced to settle. Consequently, air pollutants accumulate in the atmosphere. Additionally, the observed high SO₂ column density in north Durban in spring could have been due to road traffic since north Durban, as argued by [38], is primarily residential. Figure 6a shows a decrease in SO₂ hotspots compared to Figure 5a. However, SO₂ levels remained high. On the other hand, Figure 6b shows an increase in SO₂ column density despite the Level 5

lockdown, which was initiated from 26 March 2020 to 30 April 2020 (see Table 1). The observed SO₂ hotspots in the autumn of 2020 could have been the results of essential services that were operational during the Level 5 lockdown (see Table 1). An imbalance in the atmospheric chemistry may have also contributed to the increase in SO₂ along with the natural sources of SO₂ [42]. Most of south Durban experienced a decrease in SO₂ column density in the autumn of 2020 compared to the autumn of 2019 (see Figures 6b and 5b, respectively). This can be attributed to the Level 5 lockdown, as only essential industries were operational. Additionally, the movements of vehicles were highly restricted (see Table 1). The winter of 2020 shows a decrease in SO₂ hotspots (see Figure 6c). However, SO₂ levels remained slightly elevated. In comparison to the JJA of 2019 (see Figure 5c), the JJA of 2020 had decreased SO₂ levels (see Figure 6c). The decrease in SO₂ levels in the winter of 2020 could have been due to the Level 3 lockdown, as most economic activities were not operational (see Table 1). An increase in SO₂ was observed in the spring of 2020 in both the far south and the far northern areas of Durban (see Figure 6d). This increase could have been due to the easing of lockdown restrictions from Level 3 to Level 1 (see Table 1), by which time almost all industries were operational. However, some parts of north and south Durban showed a decrease in SO₂ column density in the spring of 2020 compared to the spring of 2019 (see Figures 6d and 5d, respectively). This could mean that even though lockdown measures were on Level 1, the lockdown measures still had an impact on SO₂ levels since the Level 1 that was implemented in 2020 had some economic activities curtailed [18,39]. Additionally, the prevailing high-intensity winds in spring may have played a role in the reduction in SO₂ column density. Comparing the summer of 2020 to the summer of 2021 (see Figures 7a and 6a, respectively), the summer of 2021 did not have a plethora of SO₂ hotspots; however, SO₂ emissions remained high (see Figure 7a). This could have been the result of the increase in lockdown measures from Level 1 to Level 3 in the summer of 2021 (see Table 1). An increase in SO₂ column density is observed in south Durban in the autumn of 2021 compared to the autumn of 2020 (see Figures 7b and 6b, respectively). This could have been due to the easing of lockdown measures from Level 3 to Level 1 during the autumn of 2021. In contrast, the winter of 2021 showed a decrease in SO₂ hotspots; however, SO₂ remained high (see Figure 7c). The decrease in SO₂ hotspots in the winter of 2021 could have been due to the increase in lockdown measures from Level 2 to Level 4. By comparing the winter of 2021 and autumn of 2021, an increase in SO₂ can be observed in winter in north Durban (see Figure 7c,b, respectively). This increase in SO₂ column density in north Durban could be attributed to low temperatures and low wind velocity prevailing in winter. The lockdown restrictions were on Level 3, which means that numerous economic activities were operational; therefore, an increase in SO₂ would be expected. Additionally, domestic combustion may have also contributed. The spring of 2021 shows a slight decrease in SO₂ levels in south Durban and a major increase in north Durban, as shown in Figure 7d. These increases could have been due to the transport and light industry occurring in north Durban since lockdown measures were eased to Level 1, meaning that every economic operation was then returned to normal. A slight increase is observed at the Port of Durban during the spring of 2021 (see Figure 7d). This could have been due to the easing of lockdown measures to Level 1 where water transport was then permitted to be operational along with aircraft. Therefore, the port was back to its normal operational basis. Only a few parts of south Durban showed a decrease in SO₂ column density, which could have been due to meteorological conditions, such as high-velocity winds and high temperatures, which reduce the accumulation of air pollutants.

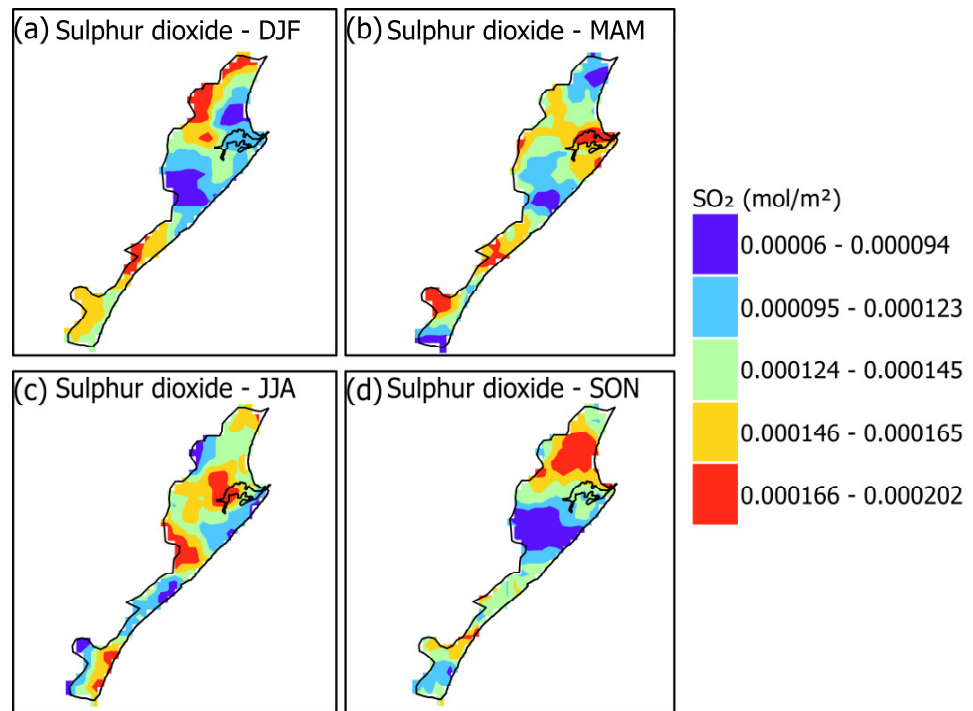


Figure 5. Sulphur dioxide column density during (a) DJF (December–January–February), (b) MAM (March–April–May), (c) JJA (June–July–August), and (d) SON (September–October–November) for 2019.

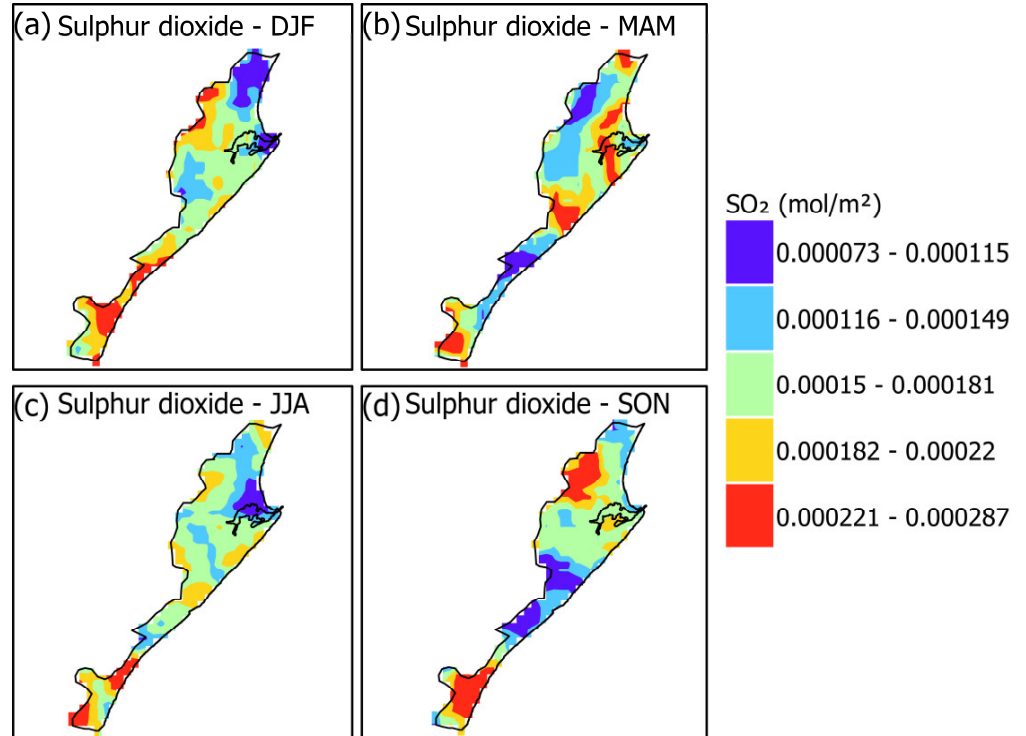


Figure 6. Sulphur dioxide column density during (a) DJF (December–January–February), (b) MAM (March–April–May), (c) JJA (June–July–August), and (d) SON (September–October–November) for 2020.

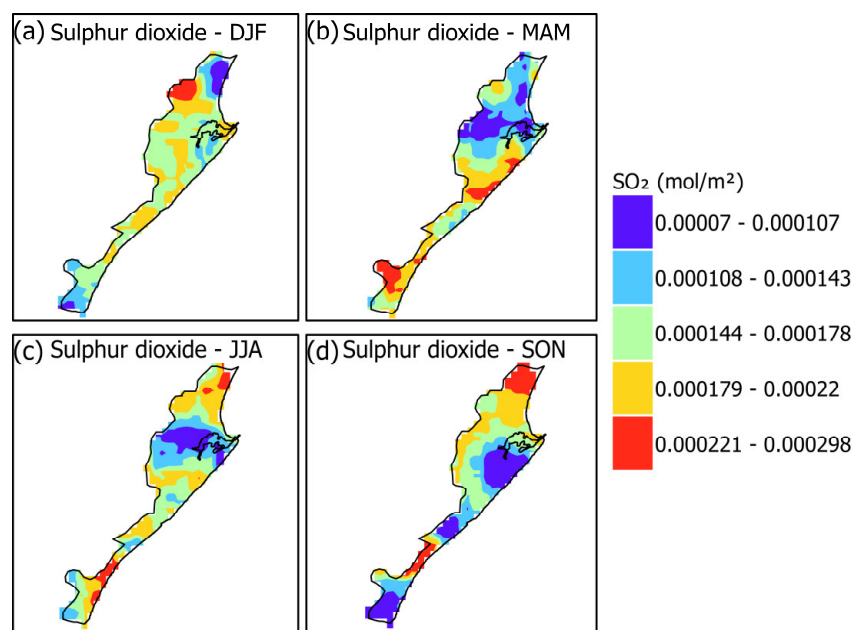


Figure 7. Sulphur dioxide column density during (a) DJF (December–January–February), (b) MAM (March–April–May), (c) JJA (June–July–August), and (d) SON (September–October–November) for 2021.

3.1.3. NO₂

Nitrogen dioxide (NO₂) is a reddish-brown gas that is formed during the high-temperature combustion of fossil fuels [2,43]. This gas is usually emitted from vehicles and industries [43]. The Durban Climate Change Society [44] argues that NO₂ from vehicles is prevalent in Durban. This argument by the Durban Climate Change Society [44] agrees with Matandirotya and Burger [22] that NO₂ is prevalent in urban areas. In 2019, Durban had a total GHG emission contribution of 41%, 31%, and 13% from road transport, industry, and residences, respectively [44]. This shows the significant contribution of road transport to the GHG emissions in Durban. Figure 8 shows NO₂ column density in Durban during 2019 on a seasonal basis. The NO₂ column density of 2019 seems to have had a similar pattern throughout the year. Conversely, only in the spring of 2019 was there a notable change compared to other seasons since the NO₂ hotspot appeared to abate (see Figure 8d). This could have been due to the prevailing strong winds and high temperatures during the spring season.

As a result, solar radiation causes photochemical reactions to occur at a higher rate, thereby reducing atmospheric NO₂. The process occurs when solar radiation detaches NO₂ after which O₃ is eventually formed [22,45]. The observed pattern of NO₂ column density was the highest in the Durban Central Business District (CBD), which could have been due to road traffic since CBDs usually have significant movement of road traffic [22]. The summer of 2020 showed an increase in NO₂ column density in north Durban (see Figure 9a). Ref. [46] argue that people visit Durban frequently during the summer months. Therefore, it is reasonable to argue that Durban road traffic volume becomes prominent during summer, and thus, a high NO₂ column density occurs. The NO₂ hotspot was reduced in the autumn of 2020 compared to the summer of 2020 (see Figure 9b,a, respectively). Furthermore, the autumn of 2020 showed a less pronounced NO₂ hotspot compared to the autumn of 2019 (see Figure 9b and 8b, respectively). This decrease in NO₂ column density in the autumn of 2020 can be attributed to the Level 5 lockdown measures, which halted almost all economic activity, including all modes of transport (see Table 1). Subsequent to the easing of lockdown measures from Level 5 to Level 4, an increase in NO₂ column density was observed in the winter of 2020 (see Figure 9c). Additionally, the increase in NO₂ column density observed in Figure 9c could be attributed to cloudy conditions and

low temperatures during the winter months. Ref. [38] argue that cloudy skies and low temperatures reduce photochemical reactions because of limited solar radiation. Ref. [46] further argue that the inversion layer is preponderant during winter months in Durban. As a result, the inversion layer traps air pollutants near the ground surface; thus, there is increased NO_2 column density. During the spring of 2020, NO_2 column density slightly decreased compared to the winter of 2020 (see Figure 9d,c, respectively). Conversely, lockdown measures were eased to Level 1 during the spring of 2020 where we would anticipate the NO_2 column density to increase. This slight decrease in NO_2 column density in the spring of 2020 could be accounted for by the high prevailing wind velocities and high temperatures, which at the local level dilute air pollutants in the atmosphere. Regardless of the prevailing high temperatures, the summer of 2021 showed an increase in NO_2 column density, as seen in Figure 10a. Thus, one can argue that high humidity in summer plays a role in increasing NO_2 column density.

This is because high humidity means more water vapour in the air; consequently, it makes the air heavy, thus causing air pollutants to settle down [47]. Figure 10b shows that the autumn of 2021 had a decrease in NO_2 column density compared to the autumn of 2019. Although it was during Level 1 lockdown measures, the impacts of lockdown measures can be noticed since only a few economic activities were allowed to operate. The winter of 2021 experienced most of the Level 3 and Level 4 lockdown measures. Despite stricter lockdown measures, an increase in NO_2 column density was observed during the winter of 2021 (see Figure 10c). This could be attributed to the prevalence of inversion layers during winter, as argued by [46]. Additionally, low wind speed, cloudy weather conditions, and low temperatures may have also contributed to the accumulation of NO_2 in the atmosphere. This is because the low wind speed decreases the rate of air pollutants' dispersion, whereas cloudy conditions and low temperatures reduce the rate of photochemical reaction [38,46]. Consequently, NO_2 accumulates in the atmosphere. On the contrary, during the spring of 2021 when high wind speed and high temperatures are prominent, a decrease in NO_2 column density was observed (see Figure 10d). High wind speed and high temperatures may have played a role in reducing the accumulation of NO_2 in the atmosphere. Ref. [38] argue that wind direction also plays a vital role in influencing the accumulation of air pollutants in the atmosphere. In addition, Ref. [22] argue that southwesterly winds are prominent in Durban. This could mean that NO_2 dominating in north Durban was influenced by the southwesterly winds.

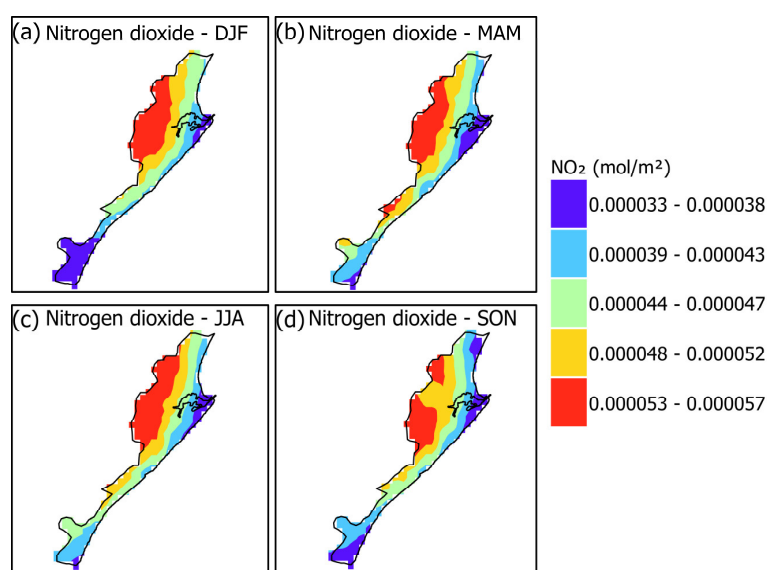


Figure 8. Nitrogen dioxide column density during (a) DJF (December–January–February), (b) MAM (March–April–May), (c) JJA (June–July–August), and (d) SON (September–October–November) for 2019.

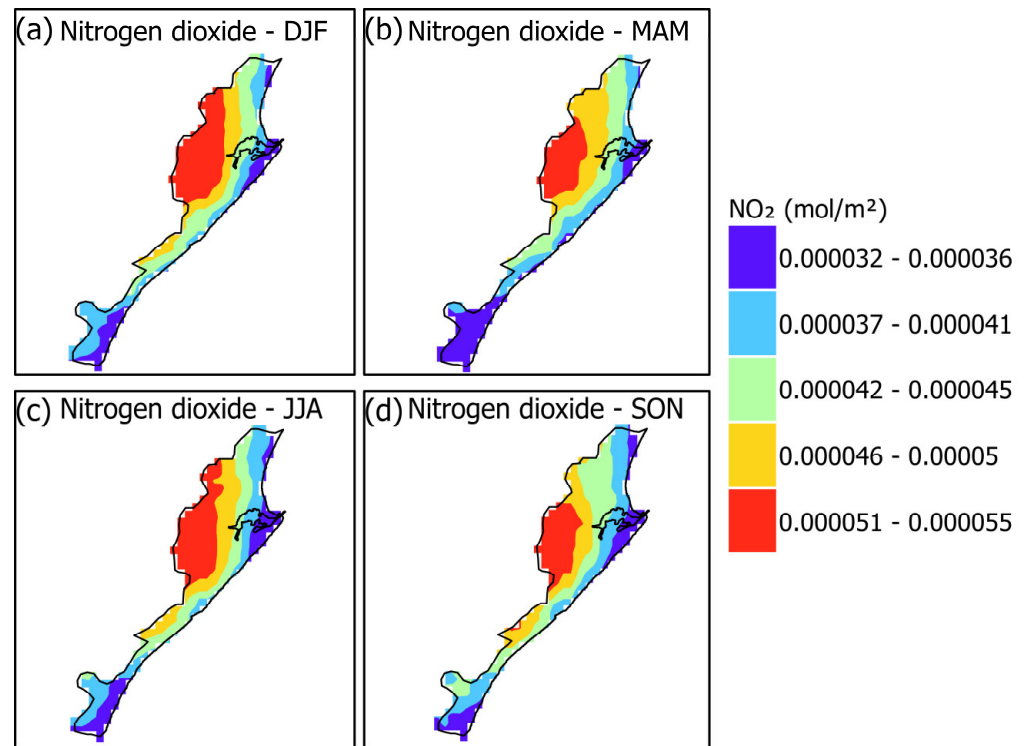


Figure 9. Nitrogen dioxide column density during (a) DJF (December–January–February), (b) MAM (March–April–May), (c) JJA (June–July–August), and (d) SON (September–October–November) for 2020.

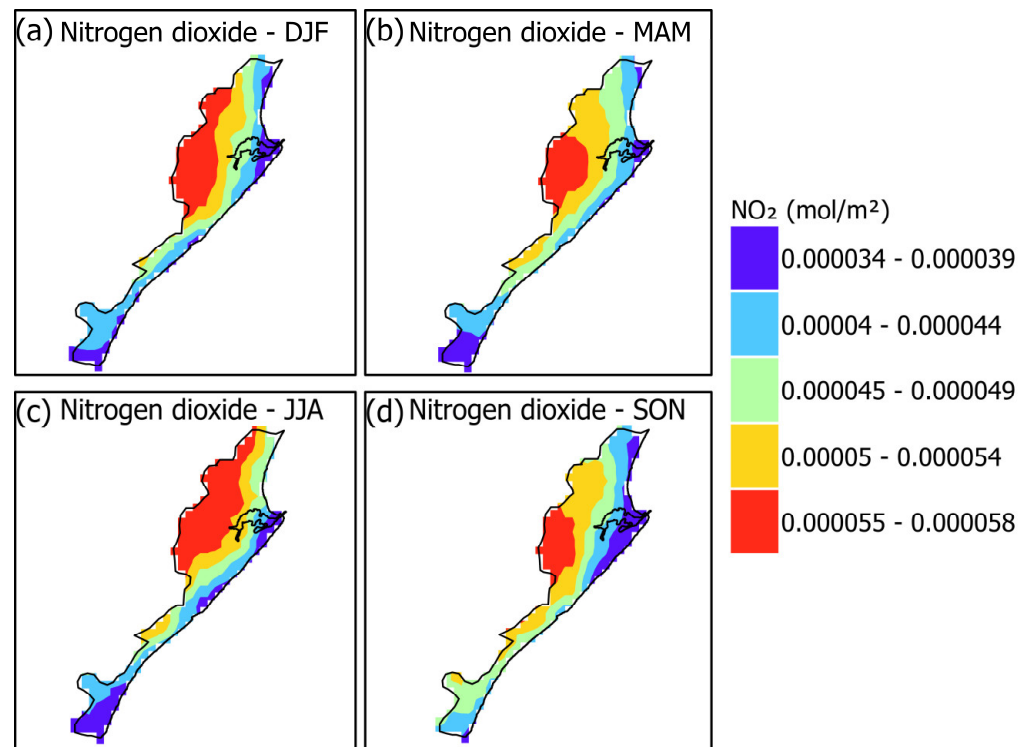


Figure 10. Nitrogen dioxide column density during (a) DJF (December–January–February), (b) MAM (March–April–May), (c) JJA (June–July–August), and (d) SON (September–October–November) for 2021.

3.2. Sequential Mann–Kendall

3.2.1. CO

The SQMK trends are presented below in Figures 11–13, with the red line representing the progressive/forward series, whereas the retrograde/backward series is represented by the light blue line. The confidence interval for this test is set at $\alpha = 0.05$ (± 1.96). The upper bound (+1.96) is represented by the solid black line, whereas the lower bound (-1.96) is represented by the square dotted black line. The point at which the red line and the light blue line intersect indicates an abrupt change and the month in which the change occurred. A significant trend is observed when the progressive series cross the lower or upper bounds, whereas an insignificant trend is observed when the progressive series is within both the upper and lower bounds. Figure 11a represents CO column density in 2019. An insignificant decrease in CO column density is portrayed by a turning point that occurred from December 2018 to January 2019 (see Figure 11a). Additionally, an insignificant increase in CO column density in February 2019 was observed; this increase became significant in April 2019 (see Figure 11a). The increase in CO column density could have been due to road traffic and poor air pollution control. The progressive series continued the significant increase in CO column density from April 2019 to August 2019, when there was a significant decrease in CO column density until November 2019 (see Figure 11a).

The significant increase in CO during the winter months could have been due to increased domestic burning of fossil fuels. Moreover, low wind speed, cloudy skies, and low temperatures could have contributed to the increased accumulation of air pollutants in the atmosphere [22,38]. In contrast, an insignificant increase in CO column density occurred from December 2019 to March 2020 and was followed by an abrupt increase in January 2020 (see Figure 11b). This increase in CO column density is relatively common in the summer months and can be accounted for by the influx of vehicles travelling to Durban for the summer holidays. Furthermore, a turning point is observed from March 2020 to April 2020, which shows there was a decrease in CO column density (see Figure 11b). This decrease can be attributed to the Level 5 lockdown (see Table 1). An increase in CO column density is observed from April 2020, but this only became significant in May 2020; the significant CO column density lasted until July 2020 (see Figure 11b). This increase can be accounted for by the easing of lockdown restrictions at that time (see Table 1). A significant decrease in CO column density followed from July 2020 to October 2020 (see Figure 12b). This decrease can be accounted for by the high wind speeds, clear skies, and high temperatures during spring, which can reduce the accumulation of air pollutants in the atmosphere. Figure 11c shows a decrease in NO₂ column density from December 2020 to February 2021. This decrease could have been due to the increase in lockdown measures that took place from Level 1 to Level 3 (see Table 1). However, the decrease was insignificant as it falls within the set threshold ($\alpha = 0.05$). An insignificant increase is observed in February 2021 (see Figure 11c). This increase in CO column density can be attributed to the easing of lockdown measures from Level 3 to Level 1 (see Table 1). The increase in CO column density in February 2021 continued until it became significant in June 2021 and lasted until August 2021 (see Figure 11c).

The significant increase in CO column density in June can be attributed to winter weather conditions, such as cloudy skies and low temperatures, which influence the accumulation of air pollutants. A significant decrease in CO column density followed from August 2021 to October 2021, when the decrease in CO column density started being insignificant until November 2021 (see Figure 11c). This decrease in CO column density can be attributed to the prevalence of gusty winds and high temperatures in spring, which help to reduce the accumulation of air pollutants in the atmosphere.

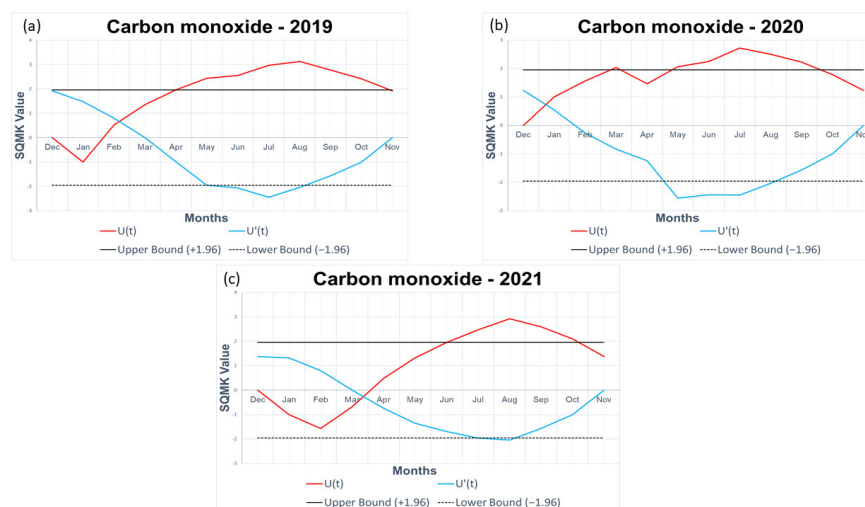


Figure 11. SQMK trends showing carbon monoxide column density in Durban: (a) CO column density during 2019, (b) CO column density during 2020, and (c) CO column density during 2021.

3.2.2. SO₂

Figure 12 represents SO₂ column density from 2019 to 2021. Figure 12a shows SO₂ column density in 2019; it shows that there was an insignificant decrease in SO₂ column density in December 2018, followed by a turning point extending the insignificant decrease in SO₂ column density until February 2019. This decrease may have been due to the precipitation and gusty winds prevailing in the summer seasons. As a result, these meteorological conditions reduce the accumulation of air pollutants in the atmosphere [22]. February 2019 shows an insignificant increase in SO₂ column density, which is followed by an abrupt increase in April 2019 that extended the increase (see Figure 12a). This insignificant increase in SO₂ column density continued until July 2019 (see Figure 12a). Consequently, the increase in SO₂ column density until July 2019 could have been due to the high domestic combustion of fossil fuels for interior heating. Additionally, cloudy skies and low temperatures dominating at that time may have played a role in increasing SO₂ column density in the atmosphere. An insignificant decrease in SO₂ column density followed from August 2019 to November 2019 (see Figure 12a). As a result, this spring decrease in SO₂ column density could have been due to the high wind speeds prevailing, which in turn reduced the accumulation of air pollutants in the atmosphere.

Briefly stated, both the increase and decrease in SO₂ column density observed in Figure 12a were insignificant. A further insignificant decrease in SO₂ column density was observed until December 2019, and then an insignificant increase in SO₂ column density occurred again in January 2020 (see Figure 12b). This can potentially be accounted for by the prominence of high rates of people travelling to Durban for the summer holidays (with an associated increase in road traffic). Additionally, a lack of SO₂ sinks may have also played a role in the increase in SO₂ column density. An abrupt change occurred in March 2020, followed by a turning point, which showed a decrease in SO₂ column density (see Figure 12b). This decrease can be attributed to Level 5 lockdown measures (see Table 1). However, this insignificant decrease lasted until April 2020 and was followed by an abrupt increase in SO₂ column density until July 2020 (see Figure 12b). Harper et al. [48] argue that accelerated levels of SO₂ were observed in Durban after the easing of lockdown restrictions to Level 4. Surprisingly, despite the further easing of lockdown measures to Levels 3 and 2, where we would expect an increase in air pollution, a decrease in SO₂ column density was observed from July 2020 to November 2020 (see Figure 12b). However, the decrease in SO₂ column density was not significant. The decrease in SO₂ column density during the spring of 2020 could have been due to better air pollution control and an increase in the availability of SO₂ sinks. A further decrease in SO₂ column density was observed in December 2020, and it was followed by a turning point, which furthered the decrease in SO₂ column density

(see Figure 12c). This summer decrease in SO₂ column density could have been due to the increase in lockdown measures from Level 1 to Level 3 (see Table 1), assisted by gusty winds and high temperatures that might have reduced SO₂ column density.

An abrupt increase was observed in March 2021, followed by an increase in SO₂ column density, as observed in Figure 12c. This may have been due to the easing of lockdown restrictions from Level 3 to Level 1 (see Table 1). This increase in SO₂ column density was insignificant, although this was followed by a short-duration significant increase in SO₂ column density for June–July 2021 (see Figure 12c). This significant increase in SO₂ column density in winter may be attributed to increased domestic combustion of fossil fuels, the prevalence of cloudy skies, and less intense winds, which increase the accumulation of air pollutants. A decreasing significant trend was observed from August 2021 to September 2021, and an insignificant decreasing trend followed from October 2021 to November 2021 (see Figure 12c). This decrease could have been due to the prevailing gusty winds, which could have reduced the accumulation of air pollutants during the spring months.

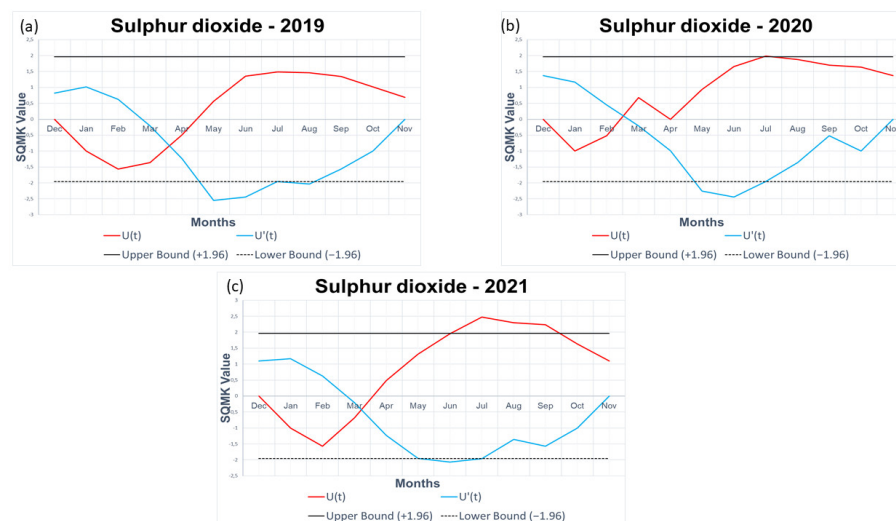


Figure 12. SQMK trends showing sulphur dioxide column density in Durban: (a) SO₂ column density during 2019, (b) SO₂ column density during 2020, and (c) SO₂ column density during 2021.

3.2.3. NO₂

Figure 13 shows the NO₂ column density in Durban from 2019 to 2021. Figure 13a shows that NO₂ column density had an insignificant increase from January 2019 to February 2019. An increase in NO₂ column density could have been due to the prominence of vehicles that travel to Durban for summer holidays, which exacerbated existing high road traffic emissions. An insignificant decrease begins from February 2019 to April 2019, and then a long insignificant increasing trend is observed until July 2019 (see Figure 13a). This is then followed by an insignificant decrease from July 2019 to December 2019, as seen in Figure 13a. This decrease in NO₂ column density is likely to be due to high temperatures and high precipitation rates in spring months, which increase the photochemical reaction of NO₂. The photochemical reaction of sunlight + NO₂ ends up forming O₃, and the reaction of H₂O + NO₂ in the atmosphere forms acid rain as far as the research stretches [22,49]. As a result, the accumulation of NO₂ in the atmosphere reduces. In contrast, Figure 13b shows an increase in NO₂ column density from January 2020 to March 2020. This could have been due to the free movement of road traffic and fully functional industries prior to the first lockdown measures.

A decrease in NO₂ column density was observed from March 2020 to April 2020 when COVID-19 struck South Africa (see Figure 13b and Table 1). This observed decrease in NO₂ column density may have been due to the restrictions on economic activities,

including free movement of road traffic (see Table 1). An insignificant increase in NO_2 column density was observed from April 2020 until it became significant in June 2020 (see Figure 13b). This significant increase in NO_2 column density in winter could have been due to low temperatures and less precipitation, which influence the accumulation of NO_2 in the atmosphere. Additionally, the easing of lockdown restrictions from Level 4 to Level 3 may have contributed to the increase in NO_2 column density in the winter of 2020 (see Table 1). A significant decrease in NO_2 column density occurred from July 2020 to August 2020 (see Figure 13b). This decrease in column density was followed by an insignificant decrease, which continued until December 2020 (see Figure 13b). The subsequent decrease in NO_2 column density can be ascribed to high wind speeds and increased solar radiation, which in turn decrease NO_2 in the atmosphere by influencing photochemical reactions and increasing the dispersion of NO_2 [22,43].

Additionally, Level 1 lockdown measures that were implemented from September 2020 to October 2020 allowed less activity compared to Level 1 lockdown measures that were implemented in 2021 [18]. Thus, some of the economic activities were inactive from September 2020 to October 2020 but thereafter, recommenced activity may have contributed to the decrease in NO_2 column density in the spring and early summer of 2021. Figure 13c below shows a further decrease in NO_2 column density from January 2021 to February 2021. This decrease in NO_2 column density could have been due to the increase in lockdown measures from Level 1 to Level 3, as seen in Table 1. In this case, the road traffic influx that usually occurs during the summer months in Durban was limited. An insignificant increase in NO_2 column density is observed from February 2021 to June 2021, when it became significant for a short period (see Figure 13c). This increase in NO_2 column density could have been due to the easing of lockdown measures (see Table 1).

A slight significant decrease in NO_2 column density is observed in July 2021 (see Figure 13c). This is followed by an insignificant decrease in NO_2 column density from August 2021 to October 2021, and then a turning point was formed, furthering the decrease in NO_2 column density, which was also not significant. The short significant decreasing trend of NO_2 column density in July 2021, as seen in Figure 13c, can be attributed to the increase in lockdown measures to Level 4, as the measures were implemented for a short time only (see Table 1). Despite Level 1 lockdown measures being implemented in October 2021, a decreasing trend in NO_2 column density is observed (see Figure 13c). This can be attributed to the prevalence of high temperatures and high-intensity winds, which reduce the accumulation of air pollutants. Therefore, there was a balance between NO_2 sources and sinks.

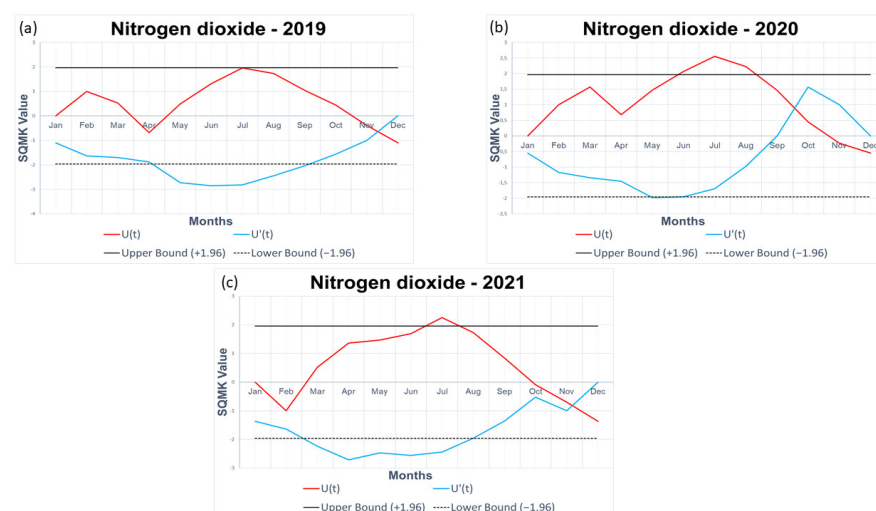


Figure 13. SQMK trends showing nitrogen dioxide column density in Durban: (a) NO_2 column density during 2019, (b) NO_2 column density during 2020, and (c) NO_2 column density during 2021.

4. Discussion

Durban was chosen as a study area because as a city, it contributes significantly to the country's GHG emissions [2]. Furthermore, cities host industries, including manufacturing, and experience significant traffic movement. Durban, furthermore, hosts the two largest petroleum refineries in South Africa, the busiest port in Africa, and is the country's major vehicle manufacturing centre. Additionally, it has large-scale chemical industries [2,44]. In response to the COVID-19 pandemic, and to reduce and manage the COVID-19 infection rates, the South African government implemented lockdown measures. The COVID-19 lockdown measures disrupted the economic activities of the country, including the city of Durban. In a study conducted by Bashir et al. [13], the decrease in economic activities associated with COVID-19 significantly reduced air pollution. Similarly, a study conducted by Filonchyk [10] in East China showed that the COVID-19-associated decrease in economic activities led to a decrease in air pollution. This paper has discussed the sources and sinks of CO, SO₂, and NO₂; however, it did not incorporate sources and sinks in the results. Sources and sinks were discussed in detail to acknowledge that there may have been other factors that affected air pollution that were beyond the control of the COVID-19 lockdown restrictions.

This study shows that the SDIB is the most polluted area of Durban, which could be attributed to the high industrialisation in the SDIB. Additionally, this study shows that CO column density in south Durban is higher than north Durban. Conversely, this study further shows that SO₂ and NO₂ column densities for north Durban are higher than south Durban. The high NO₂ and SO₂ in north Durban could be the result of pollution from road transportation, and domestic combustion since north Durban is largely a residential area. Furthermore, the broader area of north Durban is subject to the effects of agricultural burning. Additionally, north Durban is the home of the CBD; therefore, road traffic is expected to be high. However, a short-period decrease was observed in all investigated pollutants during Level 5 lockdown measures. Furthermore, an abrupt increase was observed in all investigated pollutants when the lockdown measures were eased to Level 4. Similarly, a study conducted in Gauteng (South Africa) by Shikwambana and Kganyago [11] shows that there was a reduction in air pollution during Level 5 lockdown. However, an abrupt increase was observed immediately after Level 5 lockdown measures were eased to Level 4 lockdown measures. Perhaps, if Level 5 lockdown measures had been extended, then a significant decreasing trend would have been observed in this study. However, extended Level 5 lockdown measures are not possible, as they would have caused an economic catastrophe. With that being noted, as shown by Shikwambana and Kganyago [11] and as argued by Filonchyk [10], economic activities have a direct connection with air pollution. The investigated pollutants in this study all showed an increase in the winter and a decrease in the spring. The increase in the winter could have been due to the meteorological conditions that generally prevail at that time of the year (June, July, and August), such as the presence of the inversion layer, low temperatures, and low wind speed, which in turn influence air pollutant accumulation in the atmosphere. In contrast, the decrease in spring observed in this study could have been due to the prevalence of high wind speed, high temperatures, and clear skies that generally occur at that time of year (spring until autumn). In other words, these meteorological conditions in spring, summer, and autumn allow the dispersion of air pollutants and high rates of photochemical reactions. Thus, there is usually a reduced accumulation of air pollutants in the atmosphere during those seasons.

The SQMK test was used in this study to detect if there were any significant changes caused by the COVID-19 lockdown measures in the trends of the investigated air pollutants. In this regard, the SQMK results showed that COVID-19 lockdown measures did not cause any significant changes in CO, NO₂, and SO₂ trends. Therefore, based on the SQMK test, this study failed to reject the null hypothesis. Nevertheless, the results indicated that if strict regulations could be implemented on human activities, air pollution could be reduced. However, it is not feasible to reduce air pollution by simply halting economic activity,

as the quality of life of the population depends on many economic activities occurring. Further, if the world moved swiftly from coal-fired power stations to green energy, the communities reliant on work in coal mines will be affected. Therefore, in terms of meeting the Sustainable Development Goals, governments and states need to consider both the environmental and societal aspects. Air pollution is a conundrum in South Africa. Over 2 000 deaths occur in South Africa annually due to air pollution [47]. This indicates that the air pollution laws and regulations in South Africa are not being followed, and people's lives, including the environment, are susceptible to harm. As South Africa is part of the UNFCCC, it seems that the existing laws that control air pollution are not sufficient to ensure a reduction in GHG emissions.

5. Conclusions

This research report has used various satellite sensors including Sentinel-5P, OMI, AIRS, and MERRA 2 reanalysis data to study the spatial and temporal variations of CO, SO₂, and NO₂ in Durban. The data on the investigated pollutants were collected before, during, and after high COVID-19 lockdown measures. The analysis was performed to show the impacts of COVID-19 lockdown measures on CO, NO₂, and SO₂ trends in Durban. The SQMK showed no significant trends for all investigated gases. Level 5 lockdown measures showed notable changes in the CO, NO₂, and SO₂ trends; however, the observed reductions during Level 5 lockdown measures were not significant. Additionally, an abrupt increase was observed in all investigated air pollutants when COVID-19 lockdown measures were eased to Level 4 lockdown measures. All the investigated gases showed an increase in winter, which could be ascribed to meteorological conditions such as low temperatures, low wind speed, and less precipitation, which influence the accumulation of air pollutants in the atmosphere. In contrast, a decrease was observed in all investigated gases during spring months, which was ascribed to gusty winds, high temperatures, and high precipitation, which assist in reducing the accumulation of air pollutants in the atmosphere. Outside of the meteorological factors, this study showed that a firm control of human activities could assist to abate air pollution. The lack of meteorological data and data from direct emission sources limited this study; we recommend that future studies could reinforce them.

Author Contributions: Conceptualisation, B.M., P.M. and L.S.; methodology, B.M., P.M. and L.S.; software, B.M.; formal analysis, B.M.; investigation, B.M.; writing—original draft preparation, B.M.; writing—review and editing, P.M. and L.S. All authors have read and agreed to the published version of the manuscript.

Funding: This research received no external funding.

Institutional Review Board Statement: Not applicable.

Informed Consent Statement: Not applicable.

Data Availability Statement: The datasets used in this study were obtained from open sources including Giovanni, <https://giovanni.gsfc.nasa.gov/giovanni/> (accessed on 15 August 2023), and Google Earth Engine, <https://code.earthengine.google.com/> (accessed on 15 August 2023).

Acknowledgments: The authors would like to extend their gratitude to the European Space Agency (ESA) for providing Sentinel-5p data. The author acknowledges the GES-DISC Interactive Online Visualization and Analysis In-fra-structure (Giovanni) for providing the AIRS, OMI, and MERRA-2 data.

Conflicts of Interest: The authors declare no conflict of interest.

References

1. Shikwambana, L.; Kganyago, M.; Mhangara, P. Temporal analysis of changes in anthropogenic emissions and urban heat islands during COVID-19 restrictions in Gauteng province, South Africa. *Aerosol Air Qual. Res.* **2021**, *21*, 200437. [CrossRef]
2. Jagarnath, M.; Thambiran, T. Greenhouse gas emissions profiles of neighbourhoods in Durban, South Africa—an initial investigation. *Environ. Urban.* **2018**, *30*, 191–214. [CrossRef]

3. Davidson, J. Air Pollution Responsible for Over 6.6 Million Deaths Worldwide in 2020, Study Finds. 21 October 2020. Available online: <https://www.ecowatch.com/air-pollution-deaths-study-2648424420.html> (accessed on 6 May 2023).
4. Venter, Z.S.; Aunan, K.; Chowdhury, S.; Lelieveld, J. COVID-19 lockdowns cause global air pollution declines. *Proc. Natl. Acad. Sci. USA* **2020**, *117*, 18984–18990. [[CrossRef](#)] [[PubMed](#)]
5. Zhang, X.; Yin, Y.; van der A, R.; Lapierre, J.L.; Chen, Q.; Kuang, X.; Yan, S.; Chen, J.; He, C.; Shi, R. Estimates of lightning NO_x production based on high-resolution OMI NO₂ retrievals over the continental US. *Atmos. Meas. Tech.* **2020**, *13*, 1709–1734. [[CrossRef](#)]
6. Chekir, N.; Ben Salem, Y. What is the relationship between the coronavirus crisis and air pollution in Tunisia? *Euro-Mediterr. J. Environ. Integr.* **2021**, *6*, 3. [[CrossRef](#)] [[PubMed](#)]
7. Diab, R.; Prause, A.; Bencherif, H. Analysis of SO₂ pollution in the South Durban Industrial Basin: Research in action. *South Afr. J. Sci.* **2002**, *98*, 543–546.
8. Newman, J.R. Effects of industrial air pollution on wildlife. *Biol. Conserv.* **1979**, *15*, 181–190. [[CrossRef](#)]
9. United Nations Environment Programme. COVID-19 Caused Only a Temporary Reduction in Carbon Emissions—UN Report. 16 September 2021. Available online: <https://www.unep.org/news-and-stories/press-release/covid-19-caused-only-temporary-reduction-carbon-emissions-un-report> (accessed on 6 May 2023).
10. Filonchik, M.; Hurynovich, V.; Yan, H.; Gusev, A.; Shpilevskaya, N. Impact assessment of COVID-19 on variations of SO₂, NO₂, CO and AOD over East China. *Aerosol Air Qual. Res.* **2020**, *20*, 1530–1540. [[CrossRef](#)]
11. Shikwambana, L.; Kganyago, M. Assessing the Responses of Aviation-Related SO₂ and NO₂ Emissions to COVID-19 Lockdown Regulations in South Africa. *Remote Sens.* **2021**, *13*, 4156. [[CrossRef](#)]
12. Kumar, A.; Singh, P.; Raizada, P.; Hussain, C.M. Impact of COVID-19 on greenhouse gases emissions: A critical review. *Sci. Total Environ.* **2022**, *806*, 150349. [[CrossRef](#)]
13. Bashir, M.F.; Jiang, B.; Komal, B.; Bashir, M.A.; Farooq, T.H.; Iqbal, N.; Bashir, M. Correlation between environmental pollution indicators and COVID-19 pandemic: A brief study in Californian context. *Environ. Res.* **2020**, *187*, 109652. [[CrossRef](#)] [[PubMed](#)]
14. Buthelezi, S.A.; Davies, T.C. Carbon monoxide (CO), ozone (O₃) and nitrogen dioxide (NO₂) exposure from vehicular transportation and other industrial activities in the vicinity of Umlazi Township, South of Durban, KwaZulu-Natal Province, South Africa. *Trans. R. Soc. South Afr.* **2015**, *70*, 277–283. [[CrossRef](#)]
15. Manglele, N.M. Evaluating the Contribution of Ship Exhaust Gas Emissions to Air Pollution and the Urban Carbon Footprint: A Case Study of Durban Port. Doctoral Dissertation, University of KwaZulu-Natal, Durban, South Africa, 2014.
16. Durban Climate Action Plan. Towards Climate Resilience and Carbon Neutrality. 2019. Available online: https://cdn.locomotive.works/sites/5ab410c8a2f42204838f797e/content_entry5c8ab5851647e100801756a3/5e5e3f71469c8b00a735fbac/files/Climate_Action_Plan_web.pdf (accessed on 3 August 2023).
17. Jury, M.R.; Buthelezi, M.S. Air Pollution Dispersion over Durban, South Africa. *Atmosphere* **2022**, *13*, 811. [[CrossRef](#)]
18. Potgieter, A.; Fabris-Rotelli, I.N.; Kimmie, Z.; Dudeni-Tlhone, N.; Holloway, J.P.; Janse van Rensburg, C.; Thiede, R.N.; Debba, P.; Manjoo-Docrat, R.; Abdelatif, N.; et al. Modelling representative population mobility for COVID-19 spatial transmission in South Africa. *Front. Big Data* **2021**, *4*, 718351. [[CrossRef](#)] [[PubMed](#)]
19. Bhatia, J. Cape Town ‘Day Zero’ Drought Risk Lurking Around the Corner: Study. Down to Earth. 17 November 2020. Available online: <https://www.downtoearth.org.in/news/climatechange/president-biden-will-put-us-back-on-obama-s-climate-trajectory-holdren-74156> (accessed on 4 August 2023).
20. Lloyd, P. Reassessment of the environmental impacts of sulphur dioxide emissions from power stations. *J. Energy S. Afr.* **2013**, *24*, 28–36. [[CrossRef](#)]
21. Jin, L.; Zhou, T.; Fang, S.; Zhou, X.; Bai, Y. Association of air pollutants and hospital admissions for respiratory diseases in Lanzhou, China, 2014–2019. *Environ. Geochem. Health* **2023**, *45*, 941–959. [[CrossRef](#)]
22. Matandirotya, N.R.; Burger, R. An assessment of NO₂ atmospheric air pollution over three cities in South Africa during 2020 COVID-19 pandemic. *Air Qual. Atmos. Health* **2023**, *16*, 263–276. [[CrossRef](#)]
23. Theys, N.; Hedelt, P.; De Smedt, I.; Lerot, C.; Yu, H.; Vlietinck, J.; Pedergnana, M.; Arellano, S.; Galle, B.; Fernandez, D.; et al. Global monitoring of volcanic SO₂ degassing with unprecedented resolution from TROPOMI on board Sentinel-5 Precursor. *Sci. Rep.* **2019**, *9*, 2643. [[CrossRef](#)]
24. Shikwambana, L.; Mokgoja, B.; Mhangara, P. A Qualitative Assessment of the Trends, Distribution and Sources of Methane in South Africa. *Sustainability* **2022**, *14*, 3528. [[CrossRef](#)]
25. Levelt, P.F.; Van Den Oord, G.H.; Dobber, M.R.; Malkki, A.; Visser, H.; De Vries, J.; Stammes, P.; Lundell, J.O.; Saari, H.; et al. The ozone monitoring instrument. *IEEE Trans. Geosci. Remote Sens.* **2006**, *44*, 1093–1101. [[CrossRef](#)]
26. Lamsal, L.N.; Krotkov, N.A.; Vasilkov, A.; Marchenko, S.; Qin, W.; Yang, E.S.; Fasnacht, Z.; Joiner, J.; Choi, S.; Haffner, D. Ozone Monitoring Instrument (OMI) Aura nitrogen dioxide standard product version 4.0 with improved surface and cloud treatments. *Atmos. Meas. Tech.* **2021**, *14*, 455–479. [[CrossRef](#)]
27. Shikwambana, L.; Mhangara, P.; Mbatha, N. Trend analysis and first time observations of sulphur dioxide and nitrogen dioxide in South Africa using TROPOMI/Sentinel-5 P data. *Int. J. Appl. Earth Obs. Geoinf.* **2020**, *91*, 102130. [[CrossRef](#)]
28. Leppelmeier, G.W.; Aulamo, O.; Hassinen, S.; Malkki, A.; Riihisaari, T.; Tajakka, R.; Tamminen, J.; Tanskanen, A. OMI very fast delivery and the Sodankyla/spl uml/Satellite Data Centre. *IEEE Trans. Geosci. Remote Sens.* **2006**, *44*, 1283–1287. [[CrossRef](#)]

29. Pagano, T.S.; Aumann, H.H.; Broberg, S.E.; Cañas, C.; Manning, E.M.; Overoye, K.O.; Wilson, R.C. SI-traceability and measurement uncertainty of the atmospheric infrared sounder version 5 level 1B radiances. *Remote Sens.* **2020**, *12*, 1338. [[CrossRef](#)]
30. Mordvin, E.Y.; Lagutin, A.A.; Revyakin, A.I. Technology of AIRS/AMSU/ATMS satellite data processing. In Proceedings of the CEUR Workshop Proceedings, Naples, Italy, 4–5 October 2021; Volume 3006, pp. 303–313.
31. Bosilovich, M.G.; Lucchesi, R.; Suárez, M. MERRA-2: File Specification. GMAO Office Note No. 9 (Version 1.1). 2016; 73p. Available online: <https://gmao.gsfc.nasa.gov/pubs/index.php?sel=on> (accessed on 8 May 2023).
32. Khatibi, A.; Krauter, S. Validation and performance of satellite meteorological dataset MERRA-2 for solar and wind applications. *Energies* **2021**, *14*, 882. [[CrossRef](#)]
33. Carmona, J.M.; Gupta, P.; Lozano-García, D.F.; Vanoye, A.Y.; Yépez, F.D.; Mendoza, A. Spatial and temporal distribution of PM_{2.5} pollution over northeastern Mexico: Application of MERRA-2 reanalysis datasets. *Remote Sens.* **2020**, *12*, 2286. [[CrossRef](#)]
34. Gelaro, R.; McCarty, W.; Suárez, M.J.; Todling, R.; Molod, A.; Takacs, L.; Randles, C.A.; Darmenov, A.; Bosilovich, M.G.; Reichle, R.; et al. The modern-era retrospective analysis for research and applications, version 2 (MERRA-2). *J. Clim.* **2017**, *30*, 5419–5454. [[CrossRef](#)]
35. Bisai, D.; Chatterjee, S.; Khan, A.; Barman, N.K. Application of sequential Mann-Kendall test for detection of approximate significant change point in surface air temperature for Kolkata weather observatory, west Bengal, India. *Int. J. Curr. Res.* **2014**, *6*, 5319–5324.
36. Chen, T.; Xia, G.; Wilson, L.T.; Chen, W.; Chi, D. Trend and cycle analysis of annual and seasonal precipitation in Liaoning, China. *Adv. Meteorol.* **2016**, *2016*, 5170563. [[CrossRef](#)]
37. Han, W.; Liang, C.; Jiang, B.; Ma, W.; Zhang, Y. Supplementary Materials: Major Natural Disasters in China, 1985–2014: Occurrence and Damages. *Int. J. Environ. Res. Public Health* **2016**, *13*, 1118. [[CrossRef](#)]
38. Tularam, H.; Ramsay, L.F.; Muttoo, S.; Naidoo, R.N.; Brunekreef, B.; Meliefste, K.; de Hoogh, K. Harbor and intra-city drivers of air pollution: Findings from a land use regression model, Durban, South Africa. *Int. J. Environ. Res. Public Health* **2020**, *17*, 5406. [[CrossRef](#)] [[PubMed](#)]
39. Sibanyoni, S. INFOGRAPHIC | Look Back at the Different Levels of COVID-19 Lockdowns in SA. SABC News. 24 June 2022. Available online: <https://www.sabcnews.com/sabcnews/infographic-look-back-at-the-different-levels-of-covid-19-lockdowns-in-sa/> (accessed on 8 May 2023).
40. Blunt, R.; Thomson, P.; Bory, O. International: The Impact of COVID-19 on the Oil & Gas Industry. Baker McKenzie. Available online: https://insightplus.bakermckenzie.com/bm/energy-mining-infrastructure_1/international-the-impact-of-covid-19-on-the-oil-gas-industry_2 (accessed on 18 June 2023).
41. Gounden, Y. Ambient Sulphur Dioxide (SO₂) and Particulate Matter (PM₁₀) Concentrations Measured in Selected Communities of North and South Durban. Doctoral Dissertation, University of Kwa-Zulu Natal, Durban, South Africa, 2006.
42. University of Liverpool. UK Lockdown and Air Pollution: Nitrogen Dioxide Halved but Sulfur Dioxide Doubled. Science Daily. 2020. Available online: <https://www.sciencedaily.com/releases/2020/09/200923124758.htm> (accessed on 27 May 2023).
43. Mkhize, P.L. Use of Air Dispersion Modelling to Determine the Impact of Gas Emissions from Coal-FIRED Boilers in South African Durban Basin. Doctoral Dissertation, Durban University of Technology, Durban, South Africa, 2020.
44. Durban Climate Change Strategy. Developing the Durban Climate Change Strategy Integrated Implementation Plans. 14 March 2022. Available online: https://www.durban.gov.za/storage/Documents/Climate/DCCS_Strategy.pdf (accessed on 8 May 2023).
45. Singh, S. A Study of the Chemical Quality of Ambient Air at Selected Intersections in the Durban Metropolis. Doctoral Dissertation, Durban Institute of Technology, Durban, South Africa, 2003.
46. Moodley, K.G.; Singh, S.; Govender, S. Passive monitoring of nitrogen dioxide in urban air: A case study of Durban metropolis, South Africa. *J. Environ. Manag.* **2011**, *92*, 2145–2150. [[CrossRef](#)] [[PubMed](#)]
47. Mokoena, K.K.; Ethan, C.J.; Yu, Y.; Quachie, A.T. Interaction effects of air pollution and climatic factors on circulatory and respiratory mortality in Xi'an, China between 2014 and 2016. *Int. J. Environ. Res. Public Health* **2020**, *17*, 9027. [[CrossRef](#)]
48. Harper, P. South Durban Chokes as Engen Refinery Starts Up. Mail and Guardian. 10 June 2020. Available online: <https://mg.co.za/environment/2020-06-10-south-durban-chokes-as-engen-refinery-starts-up/#:~:text=%E2%80%9CWhen%20the%20lockdown%20started%2C%20the,safely%20restarted%E2%80%9D%20on%20May%2016> (accessed on 10 May 2023).
49. Menezes, F.; Popowicz, G.M. Acid Rain and Flue Gas: Quantum Chemical Hydrolysis of NO₂. *ChemPhysChem* **2022**, *23*, e202200395. [[CrossRef](#)] [[PubMed](#)]

Disclaimer/Publisher's Note: The statements, opinions and data contained in all publications are solely those of the individual author(s) and contributor(s) and not of MDPI and/or the editor(s). MDPI and/or the editor(s) disclaim responsibility for any injury to people or property resulting from any ideas, methods, instructions or products referred to in the content.